Model-potential-free analysis of small angle scattering of proteins in solution: insights into solvent effects on protein-protein interaction

Tomonari Sumi[†*], *Hiroshi Imamura*[‡#], *Takeshi Morita*[‡], *Yasuhiro Isogai*[§], *and Keiko Nishikawa*[‡]

[†] Department of Chemistry, Faculty of Science, Okayama University, 3-1-1 Tsushima-Naka, Kita-ku, Okayama 700-8530, Japan.

[‡] Graduate School of Advanced integration Science, Chiba University, 1-33 Yayoi, Inage, Chiba 263-8522, Japan.

[§] Department of Biotechnology, Toyama Prefectural University, 5180 Kurokawa, Imizu, Toyama, 939-0398, Japan.

AUTHOR INFORMATION

Corresponding Author

* Email: sumi@okayama-u.ac.jp

Present Addresses

Biomedical Research Institute, National Institute of Advanced Industrial Science and Technology, 1-1-1, Higashi, Tsukuba, Ibaraki 305-8566, Japan

ABSTRACT

To extract protein-protein interaction from experimental small-angle scattering of proteins in solutions using liquid state theory, a model potential consisted of a hard-sphere repulsive potential and the excess interaction potential has been introduced. In the present study, we propose a model-potential-free integral equation method that extracts the excess interaction potential by using the experimental small-angle scattering data without specific model potential such as the Derjaguin-Landau-Verwey-Overbeek (DLVO)-type model. Our analysis of an experimental small-angle X-ray scattering data for lysozyme solution shows both the stabilization of contact configurations of protein molecules and a large activation barrier against the formation of the contact configurations in addition to the screened Coulomb repulsion. These characteristic features, which are not well-described by the DLVO-type model, are interpreted as solvent effects.

1. Introduction

Knowledge of the interactions between protein molecules in solutions is essential for understanding protein molecule's respective biological functions and predicting crystallization, which is a major step in the characterization of protein structure [1-8]. It is also important for understanding the stability of the solutions with respect to aggregation and liquid-liquid phase separation [9-13]. Small-angle scattering of X-rays and neutrons (SAXS and SANS) is an effective method to study the structure and interactions of biological macromolecules such as proteins under various conditions [14,15]. The small-angle scattering profile $I(q)$ provides a protein's interparticle interference, called the structure factor $S(q)$, and a protein's self-scattering, called the form factor, $P(q)$. $S(q)$ is related to real space information such as the pair distribution function $g(r)$ of proteins in solvent by the inverse Fourier transform. In addition, the interaction potential between proteins can be estimated using liquid-state theory. However, we cannot directly apply the inverse Fourier transform, because the experimental scattering intensity is, in fact, not available for high-scattering angle region. To deal with this, an interaction model potential such as the Derjaguin-Landau-Verwey-Overbeek (DLVO) model is widely employed. [5,6,16-21] Although the original DLVO model is expressed as the sum of only two simple interactions, screened Coulomb repulsion and van-der-Waals attraction, [22,23] for applications in a wide variety of systems, the attractive interaction in the DLVO model is often replaced with the Yukawa-type potential with variable parameters in order to take into account not only the van-der-Waals interaction but also the part of the other interactions, for instance, the solvent-induced interactions.[18] In fact, the DLVO model with the Yukawa-type attraction, referred to as "DLVO-type" in this paper, has been widely applied to reproduce the structure factor $S(q)$ of colloidal and protein solutions using liquid-state theory, [16-20,24,25] because the DLVO-type model has

empirically been well known as a minimal model that provides a good description for protein-protein interaction potential. However, the assumption underlying this model, by which the specific model potentials are introduced, would certainly limit the variety of protein-protein interactions. In fact, the necessity of non-DLVO interactions for protein solutions with high ionic strength has been reported. [6,10,26-28] Nevertheless, the concrete shape or a function form of the non-DLVO interaction is not almost clarified yet.

For gaining insight into the characteristic features of protein-protein interaction in solutions without assuming specific model potential functions, we propose a model-potential-free (MPF) method for extracting useful information about the interaction potential between protein molecules from small-angle scattering data of protein solutions. The usage of indirect Fourier transform (IFT) has been proposed by Fritz[29] and Fukasawa and Sato[25] as a model-potential-free analysis for deriving the pair distribution function from experimental structure factor. On the other hand, in our model-potential-free method based on liquid-state theory, protein-protein interaction potential as well as pair distribution function is numerically obtained by solving an integral equation without any functions for the excess interaction potential. The experimental structure factor is used as the input. On the basis of the protein-protein interaction potential calculated from the model-potential-free integral equation, we reveal the concrete shape of the non-DLVO interaction by comparing the result obtained from the DLVO-type model. In the latter half of this paper, we introduce an additional model potential for the non-DLVO interaction, and then show that it remarkably improves the DLVO-type description for the short- and middle-range interaction between protein molecules.

2. Theory

First, we introduce a hard-sphere (HS) fluid as a reference system. The excess part of the direct correlation function $c(r)$ in the Ornstein-Zernike (OZ) equation [30] over $c_{\mathrm{HS}}(r)$ and that of $V(r)$ over $V_{\mathrm{HS}}(r)$ are defined as $c_{\mathrm{ex}}(r)$ and $V_{\mathrm{ex}}(r)$, respectively, i.e., $c_{\mathrm{ex}}(r) \equiv c(r) - c_{\mathrm{HS}}(r)$ and $V_{\mathrm{ex}}(r) \equiv V(r) - V_{\mathrm{HS}}(r)$, where r is the distance between particles. The subscripts "HS" and "ex" denote hard sphere and excess, respectively. Next, we introduce the following assumption for $V_{\mathrm{ex}}(r)$:

$$-V_{\mathrm{ex}}(r)/k_{\mathrm{B}}T = c_{\mathrm{ex}}(r), \tag{1}$$

where k_{B} is the Boltzmann constant, and T is the thermodynamic temperature. This equation is formally the same as that for the random phase approximation (RPA) [30]. The assumption is asymptotically correct for the long-range behavior of $V_{\mathrm{ex}}(r)$. As a result, the following closure relation, in which neither $V(r)$ nor $V_{\mathrm{ex}}(r)$ explicitly appears, is obtained:

$$h(r) = \begin{cases} \exp\left[\gamma_{\mathrm{s}}(r) + B(r)\right] - 1 & r > d_{\mathrm{HS}} \\ -1 & r \le d_{\mathrm{HS}} \end{cases}, \tag{2}$$

where $B(r)$ is a bridge function; d_{HS} is the diameter of the hard-sphere fluid, i.e., the protein's effective diameter; and $\gamma_{\mathrm{s}}(r) = h(r) - c_{\mathrm{HS}}(r)$ is given by the inverse Fourier transform of

$$\hat{\gamma}_{\mathrm{s}}(q) = \hat{c}(q)/\left[1 - n_0\hat{c}(q)\right] - \hat{c}_{\mathrm{HS}}(q), \tag{3}$$

$$\hat{c}(q) = \hat{h}'(q) - \left[\hat{\gamma}_{\mathrm{s}}(q) - \hat{c}_{\mathrm{ex}}(q)\right]. \tag{4}$$

Here, q in Eqs. (3) and (4) corresponds to the scattering parameter that is defined as $q = 4\pi\sin(\theta)/\lambda$, where 2θ is the scattering angle and λ is the wavelength. In Eq. (4), $\hat{h}'(q)$ is given by

$$\hat{h}'(q)=\begin{cases}\hat{h}_{\mathrm{exp}}(q)=\left[S_{\mathrm{exp}}(q)-1\right]/n_0 & q\le q_{\mathrm{h}}\\ \hat{h}(q) & q>q_{\mathrm{h}}\end{cases}, \tag{5}$$

where $\hat{h}(q)$ is calculated using the closure relation of Eq. (2), n_0 is the number density of particle, and the subscript "exp" denotes experimental. In Eq. (5), the value of q_h should be chosen such that $\hat{h}(q)$ smoothly continues to $\hat{h}_{\mathrm{exp}}(q)$ at q_{h} for experimentally available values of q. Because $V_{\mathrm{ex}}(r)$ does not explicitly appear in Eq. (2), we can obtain $V_{\mathrm{ex}}(r)$ from $c_{\mathrm{ex}}(r)$ using Eq. (1) without any specific model potential by iteratively solving the integral equation until the Fourier transform of $h(r)$ calculated using Eq. (2) has well converged. The detail calculation procedure is shown in the electronic supplementary information (ESI). In this study, we employed the Verlet-modified bridge function $B(r)=\gamma^2(r)/\left[2+2(4/5)\gamma(r)\right]$ [31,32], as shown in Eq. (2). It is well known that the hypernetted chain (HNC) approximation ($B(r)=0$) essentially overestimates the value of $S(q)$ for small q values [30]. In general, the bridge function corrects the overestimation of $S(q)$ for small q values in the HNC approximation but does not significantly affect $S(q)$ for large q values.

3. Experiment

We performed SAXS experiment to obtain $S_{\mathrm{exp}}(q)$ values, using the beam line BL-10C, the Photon Factory (PF) of the High Energy Accelerator Research Organization (KEK), Tsukuba in Japan. The X-ray wavelength, λ, was 0.1488 nm; the camera length was 957 mm. X-ray intensities were recorded using single-photon counting X-ray detector, PILATUS 300K-W (DECTRIS Ltd., Switzerland). Lysozyme from hen egg white (Sigma Aldrich, St. Louis, MO) was dissolved in 25 mM bis-Tris buffer at pH 7. lysozyme solutions of 0.10 g/mL were measured

for one minute, which was repeated four times, and the data were averaged. To obtain the scattering of the form factor, $P_{\mathrm{exp}}(q)$, lysozyme solution of 2.6x10^{-3} g/mL, at the concentration of which $S(q)$ can be taken as 1, was measured. The exposure time was 80 minutes for decreasing noises at large q values (~1 – ~2.5 nm^{-1}), where the scattering is weak. The dilute sample was flowed to avoid the damage by X-ray radiation. The minimum and maximum q values for which the scattering intensity $I_{\mathrm{exp}}(q)$ was experimentally determined were approximately 0.3 and 3.2 nm^{-1}, respectively. In the present study, 2.76 nm^{-1} was used as the value of q_{h} in Eq. (5). We also extrapolated the data of $S_{\mathrm{exp}}(q)$ toward the low-q limit by applying a Lorenz-type function to the available data of $S_{\mathrm{exp}}(q)$ at the values of q between 0.3 and 0.5 nm^{-1}. The comparison between the raw $S_{\mathrm{exp}}(q)$ data that is obtained from dividing the raw scattering intensity $I_{\mathrm{exp}}(q)$ by the form factor $P_{\mathrm{exp}}(q)$ and its smoothed $S_{\mathrm{exp}}(q)$ data is shown in ESI.

4. Computational detail

The integral equation was solved with 4096 grid points, in which the maximum value of the radial distance was 100 nm. In all of the calculations, 2.7 nm was employed as d_{HS} in $V_{\mathrm{HS}}(r)$ according to the length of the shorter axis when the lysozyme was regarded as an ellipsoid. The number density of protein, n_0, was 4.2 × 10^{-3} nm^{-3} when the protein concentration was 0.10 g/mL (=7.0 mM). For comparison with the results obtained using the model-potential-free method, we also applied the DLVO-type model potential $V_{\mathrm{DLVO}}(r)$ to the same data of $S_{\mathrm{exp}}(q)$. $V_{\mathrm{DLVO}}(r)$ is given by a sum of $V_{\mathrm{HS}}(r)$, the screened Coulomb repulsive potential $V_{\mathrm{C}}(r)$ given in Eq. (6), and the Yukawa-type attractive potential $V_{\mathrm{A}}(r)$ given in Eq. (7).

$$V_{\mathrm{C}}(r)=\frac{Z^2e^2}{4\pi\varepsilon_0\varepsilon_{\mathrm{r}}\left(1+0.5\kappa d_{\mathrm{HS}}\right)^2}\frac{e^{-\kappa(r-d_{\mathrm{HS}})}}{r}, \tag{6}$$

$$V_{\mathrm{A}}(r)=-J_{\mathrm{A}}\left(d_{\mathrm{HS}}/r\right)e^{-(r-d_{\mathrm{HS}})/d_{\mathrm{A}}}, \tag{7}$$

Here, e is the elementary charge, ε_0 is the dielectric permittivity of the vacuum, and ε_{r} is the dielectric constant of the solvent. The parameter κ in Eq. (6) is the reciprocal Debye-Hückel screening length $\left[\left(2e^2/\varepsilon_0\right)I/\left(\varepsilon_{\mathrm{r}}k_{\mathrm{B}}T\right)\right]^{1/2}$, where I is the ionic strength that is given by $1/2\sum_i c_i z_i^2$ with the concentrations c_i and valences z_i of ions. According to titration experiments [33], we used $Z=8$ as the effective charge of the lysozyme in all calculations involving $V_{\mathrm{DLVO}}(r)$. The parameters J_{A} and d_{A} in Eq. (7) are considered unknown and were determined using nonlinear fitting of $S_{\mathrm{exp}}(q)$, and $V_{\mathrm{C}}(r)$ was uniquely determined using ε_{r}, I (or κ), and Z. The model-potential-free method does not require the physical quantities ε_{r}, κ (or I), and Z under the experimental conditions required by the DLVO-type model; this is regarded as one of the unique advantages of the present method. The HNC approximation combined with the Verlet-modified bridge function $B(r)$ was employed as the closure relation in all calculations involving $V_{\mathrm{DLVO}}(r)$.

5. Results and discussion

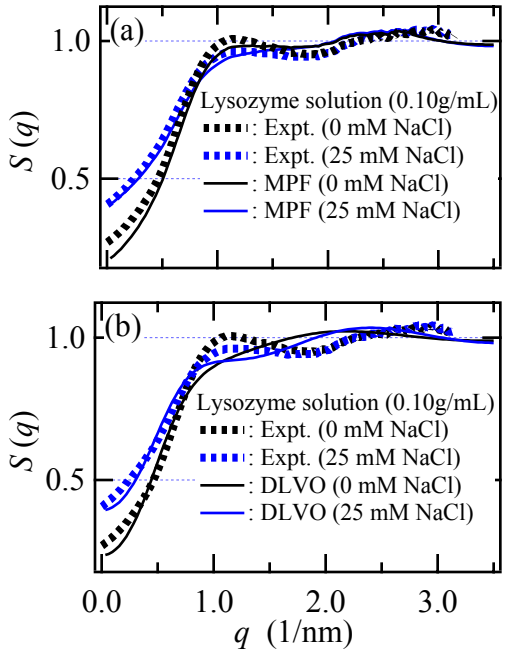

Fig. 1 Comparison between experimental and theoretical structure factors $S(q)$ for lysozyme solutions of 0.10 g/mL at 25 ºC with and without 25 mM NaCl salt in 25 mM bis-Tris buffer with pH of 7. (a) Model-potential-free (MPF) method. (b) DLVO-type model.

Figures 1(a) and 1(b) show theoretical values of $S(q)$ obtained using the model-potential-free (MPF) method and the DLVO-type model, respectively, in comparison with experimental $S_{\text{exp}}(q)$ values for lysozyme solutions of 0.10 g/mL with 0 and 25 mM concentrations of NaCl salt at 25 ºC. The characteristic two peaks observed in our experimental $S_{\text{exp}}(q)$ qualitatively agree with those that have been reported in the representative literatures.[34,35] The best-fit curves obtained by using DLVO-type model do not agree well with $S_{\text{exp}}(q)$ for large q values between 1 and 3 nm^{-1}. On the other hand, the MPF method can reproduce the characteristic features of $S_{\text{exp}}(q)$ at not only small q values but also large q values. It should be noted that the slight deviation of the MPF results from $S_{\text{exp}}(q)$ is caused by the assumption of Eq. (1). The comparison between the experimental raw $I_{\text{exp}}(q)$ and the theoretical $I(q)$ that is obtained from a product of theoretical $S(q)$ and $P_{\text{exp}}(q)$ is shown in ESI.

Pair distribution functions $g(r)$ and protein-protein interaction potentials $V(r)$ obtained using the MPF method as well as the DLVO-type model are shown in Figs. 2(a) and 2(b), respectively. At low salt concentrations, contact configurations of protein molecules are generally expected to be unstable because of the strong Coulomb repulsion by the relatively high net charge of lysozyme [33]. However, in the MPF results of $V(r)$, we find that the contact configurations between protein molecules are apparently stabilized even at 0 mM of NaCl. The stabilization of the contact configurations as a result of short-range attraction qualitatively agrees with previous works.[34,35] On the other hand, in the results of $g(r)$ for the DLVO-type model, we see the lack of short-ranged structures, i.e., the first maximum at the contact region, the first minimum, and the second maximum. The short-ranged structural information is essentially contained in the high-q data of $S_{\mathrm{exp}}(q)$, as described later (Fig. 3). The vertical rise in $g(r)$ provided by the MPF method at the contact distance would be attributed to insufficient high-q data of $S_{\mathrm{exp}}(q)$. In our preliminary application of the MPF method in which the available maximum q-value for the data of $S(q)$, i.e., q_{h}, for 0.1 g/mL lysozyme solution was 4 nm^{-1} that is quite larger than the present value of q_{h}=2.7 nm^{-1}, the position of the first maximum in $g(r)$ was shifted toward the larger distance from the contact distance and the width of the first maximum was broader.[36] The shift and the narrowing of the first maximum in $g(r)$ could be attributed to the rotational average of non-spherical lysozyme molecule. On the other hand, the vertical rise in $g(r)$ provided by the DLVO-type model is caused by an inherent feature of the DLVO-type model potential.

We show the difference between $V_{\mathrm{MPF}}(r)$ and $V_{\mathrm{DLVO}}(r)$, given as $\Delta V(r)=V_{\mathrm{MPF}}(r)-V_{\mathrm{DLVO}}(r)$, in the inset of Fig. 2(b). This difference indicates what $V_{\mathrm{DLVO}}(r)$ lacks. As discussed below, we

suggest that $\Delta V(r)$, which gives a large contribution to both the stabilization of the contact configurations and the activation barrier against the formation of the contact configurations, might be derived from the short-range attraction and the middle-range repulsion as a result of both the direct interaction between protein molecules and the solvent-induced interactions.

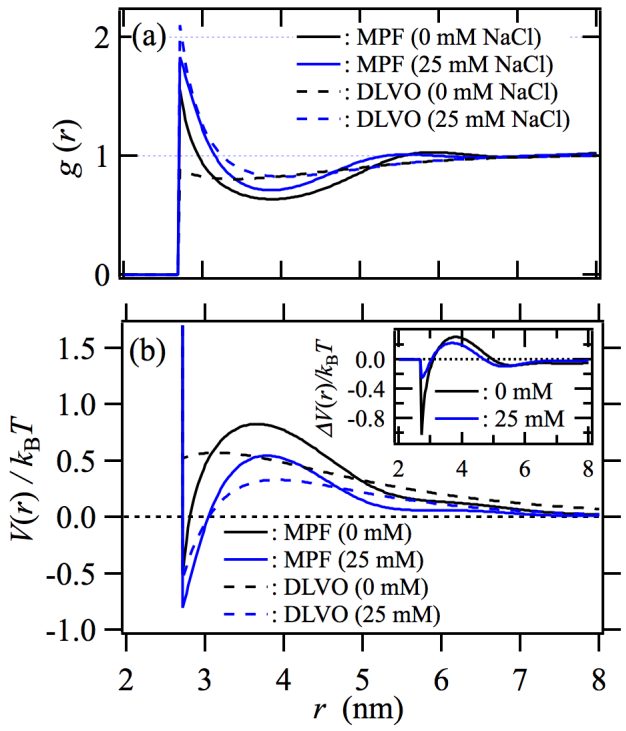

Fig. 2 (a) The pair distribution function $g(r)$ and (b) the protein-protein interaction potential $V(r)$ for lysozyme solutions of 0.10 g/mL with and without 25 mM NaCl salt at 25 ºC. In the inset of (b), the black and blue lines indicate $\Delta V(r)=V_{MF}(r)-V_{DLVO}(r)$ at 0 and 25 mM NaCl, respectively.

In our previous study of hydrophobic/solvophobic interaction between large spherical solutes such as small globular proteins [37], we showed both the stabilization of contact configurations and the activation barrier against their formation in not only a water solvent but also a Lennard-Jones (LJ) solvent. However, if the attractive interaction between the solute and solvent was fully omitted in the calculations, the activation barrier completely disappeared, and the contact configurations became stabilized. The activation barrier, in other word, the middle-range repulsion is, therefore, interpreted as the energy needed to remove water/solvent molecules in the

hydration/solvation shell surrounding the solute when the solute molecules approach each other to form the contact configurations.

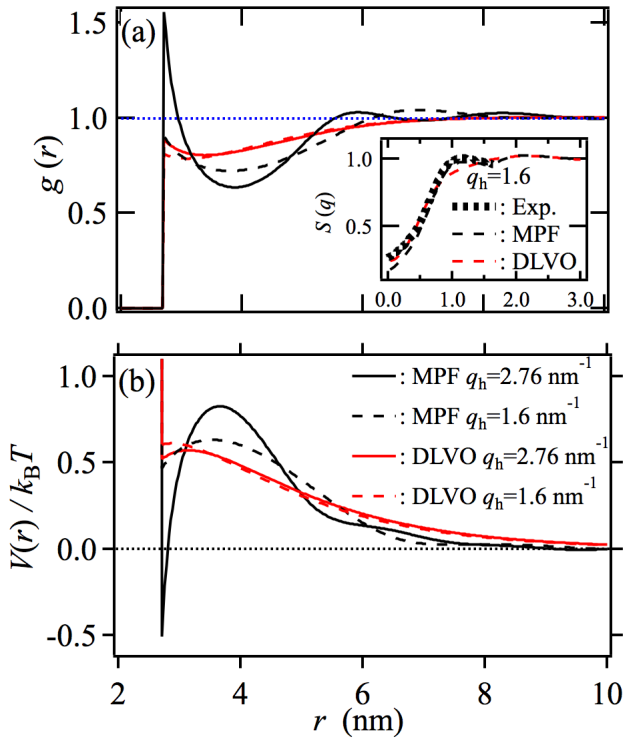

Fig. 3 q_h dependence of (a) $g(r)$ and (b) $V(r)$ obtained using the MPF method and the DLVO-type model for lysozyme solution of 0.10 g/mL without 25 mM NaCl salt. q_h is defined in Eq. (5). The black (or red) solid and broken lines indicate the MPF (or DLVO-type) results for q_h of 2.76 and 1.6 nm^{-1}, respectively. In the inset of (a), the black dotted, black broken, and red broken lines show the experimental, MPF, and DLVO-type results for $S(q)$ for q_h of 1.6 nm^{-1}.

The q_h-value dependence of $g(r)$ and $V(r)$ determined using the MPF method and the DLVO-type model are shown in Figs. 3(a) and (b), respectively. The results for q_h = 2.76 nm^{-1} in Fig. 3 are the same as the results shown in Figs. 1 and 2. $S(q)$ values obtained using the MPF and DLVO-type calculations for q_h = 1.6 nm^{-1} as well as the experimental $S_{exp}(q)$ data for q < 1.6 nm^{-1} are displayed in the inset of Fig. 3(a). The first minimum in $V(r)$ (maximum in $g(r)$) that indicates the stabilization of contact configurations disappears in the MPF result for q_h = 1.6 nm^{-1}. As pointed out by the previous works,[34,35] there are two typical length scales in the dense lysozyme solutions: the larger length scale corresponding to the first maximum in $S(q)$ arises

from the screened Coulomb repulsion and the smaller length scale corresponding to the second maximum in $S(q)$ can be assigned to the monomer-monomer contact correlation. If the high-q data of $S_{\mathrm{exp}}(q)$ were not available and then were not taken into account in the analysis, we would obtain neither the stabilization of the monomer-monomer contact configurations nor the large activation barrier against their formation. The contribution from the high-q data of $S_{\mathrm{exp}}(q)$ to the MPF result is significant, whereas the results obtained using the DLVO-type model for q_{h} values of 1.60 and 2.76 nm^{-1} are very similar to each other. The similarity between these results for both small and large values of q_{h} suggests that the DLVO-type model cannot reproduce the short- and middle-ranged structures.

As shown in the inset of Fig. 2(b), the DLVO-type model is insufficient for the description of both the stabilization of the contact configurations and the activation barrier against the formation of the contact configurations because of the limitation in the potential form of the Yukawa-type function. In order to improve the DLVO-type description of these short- and middle-ranged interactions, we introduce an additional model potential as follows:

$$V_{\mathrm{S}}(r) = -J_{\mathrm{S}}\left(d_{\mathrm{HS}}/r\right)^{\alpha} e^{-(r-d_{\mathrm{S}})^2/W_{\mathrm{S}}}. \qquad (8)$$

The physical origin of the model potential would be attributed to both the direct interaction between protein molecules and a solvent-induced interaction. If α is set as zero, $V_{\mathrm{S}}(r)$ is a Gaussian-type function involving the depth of the well J_{S}, the position of the center of the well d_{S}, and the width of the well W_{S}. In addition to the parameters J_{A} and d_{A} in Eq. (7), the parameters J_{S}, d_{S}, and W_{S} in Eq. (8) are also considered unknown and were determined using nonlinear fitting of $S_{\mathrm{exp}}(q)$. In this paper, we refer to $V_s(r)$ as "solvent-induced potential (SIP)", although not only the solvent-induced interaction but also the direct interaction between protein

molecules is included in $V_s(r)$. It is noted that we can use $V_S(r)$ to improve the DLVO-type description of both the stabilization of the contact configurations for a positive J_S and the activation barrier against the formation of the contact configurations for a negative J_S. In this study, the value of J_S was chosen to be positive so that $V_S(r)$ was a short-range attractive potential. In the previous theoretical studies, the characteristic two peaks in $S_{exp}(q)$ have been reproduced by using, for instance, a two-Yukawa model consisted of short-range attractive and long-range repulsive Yukawa-type potentials[38] and the superposition of Lennard-Jones-type potential and a Yukawa-type long-range repulsion.[39] In the case of the DLVO-type model employed in this study, one Yukawa-type potential is always fixed so that it reproduces the screened Coulomb repulsion with constant parameters and another Yukawa-type potential is used as a fitting function, whereas in the case of the two-Yukawa model,[38] both the Yukawa-type potentials are used as independent fitting functions. Therefore, the potential function in the DLVO-type model is restricted compared with the two-Yukawa model. On the other hand, in the case that the model potential of Eq. (8) is added into the DLVO-type model, the short-range attraction is mainly described by Eq. (8), thus another Yukawa-type potential can be used to improve the middle-range interaction that is mediated by hydration effects. However, in the case of the combination of Lennard-Jones-type potential and a Yukawa-type potential,[39] although the former and the latter are used as independent fitting functions for the short-range attraction and the long-range repulsion, respectively, there is no potential function to improve the middle-range repulsive interaction that also plays a crucial role on the stabilization of protein solutions.

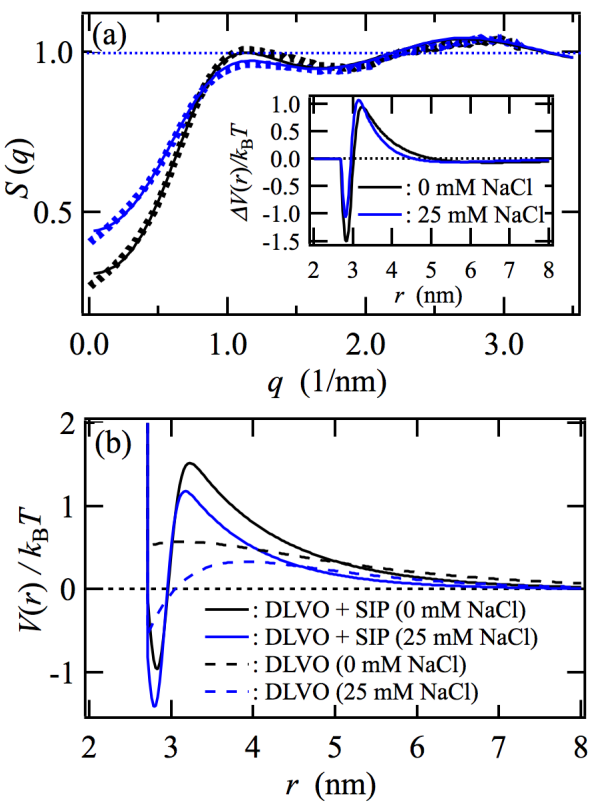

Fig. 4 (a) The black (or blue) dotted and solid lines indicate the experimental $S_{exp}(q)$s and $S(q)$s, respectively, obtained using the DLVO-type model with the solvent-induced potential (SIP) at 0 (or 25) mM NaCl. (b) The black (or blue) broken and solid lines indicate $V(r)$s obtained using the DLVO-type model and DLVO-type + SIP model, respectively, at 0 (or 25) mM NaCl. In the inset of (a), the black and blue lines indicate $\Delta V(r)=V_{SDLVO}(r)-V_{DLVO}(r)$ at 0 and 25 mM NaCl, respectively.

Figures 4(a) and 4(b) show $S(q)$ and $V(r)$, respectively, obtained using $V_{DLVO}(r)$ plus $V_S(r)$ for a positive value of J_S, i.e., $V_{SDLVO}(r)$. The value of α in Eq. (8) was set as 2.0 in the present calculation in order to take an asymmetry in $V_S(r)$ into account. When α was set as zero, we obtained results comparable with those shown in Fig. 4. The agreement with $S_{exp}(q)$ is drastically improved by the addition of $V_S(r)$ to $V_{DLVO}(r)$. The model potential $V_{SDLVO}(r)$ yields not only large stabilization of the contact configurations but also a large activation barrier against their formation. The difference defined by $\Delta V(r)=V_{SDLVO}(r)-V_{DLVO}(r)$ is displayed in the inset of Fig. 4(a). $\Delta V(r)$ in the activation barrier is not sufficiently described by the DLVO-type model even though the DLVO-type model takes into account the salt effect as the screened

Coulomb repulsion according to Eq. (6). In addition, interestingly, the salt effect yields no significant change in $\Delta V(r)$. Therefore, we suggest that the activation barrier against the formation of the contact configurations is attributed to the solvent effects on the effective protein-protein interactions.

6. Concluding remarks

In this paper, we presented the model-potential-free method for determining the excess part of the protein-protein interaction potential that is defined as the difference from an introduced hard-sphere potential by using small-angle X-ray scattering data as the input. The model-potential-free method yielded better agreement with the experimental structure factor of lysozyme solutions of 0.10g/mL at 0 and 25 mM NaCl salt concentrations compared with results obtained using the DLVO-type model potential. We also proposed an additional model potential to improve the DLVO-type description for short- and middle-ranged protein-protein interactions. The model-potential-free method and the DLVO-type potential combined with the additional model potential reproduced the characteristic features of short- and middle-ranged protein-protein interactions: the stabilization of contact configurations between protein molecules and the activation barrier against the formation of the contact configurations, which would be attributed to both the direct interaction between protein molecules and the solvent-induced interaction. We comment on the new perspective that the interaction extracted by our analysis is a possible candidate for the short-range attractive interaction, which has been regarded as the necessary factor for metastable liquid-liquid phase separation, and the physical origin of which is under debate [11,28,40-46].

ACKNOWLEDGMENT

This work was supported in part by a Grant-in-Aid for Scientific Research (KAKENHI) (No.25610121) from the Ministry of Education, Culture, Sports, Science and Technology of Japan (to T.S.) and Izumi Science and Technology Foundation (to H.I.). The SAXS experiment in this work was performed under the approval of the Photon Factory Program Advisory Committee (Proposal No. 2013P004, 2014G165). H.I. and T.S also thank Prof. Ryo Akiyama of Kyushu University for useful discussions.

REFERENCES

1. A. Tardieu, F. Vérétout, B. Krop, and C. Slingsby, *European biophysics journal*, 1992, **21**, 1–12.
2. O. D. Velev, E. W. Kaler, and A. M. Lenhoff, *Biophysical Journal*, 1998, **75**, 2682–2697.
3. B. Guo, S. Kao, H. McDonald, A. Asanov, and L. L. Combs, … *of crystal growth*, 1999.
4. F. Bonneté, S. Finet, and A. Tardieu, *Journal of Crystal Growth*, 1999, **196**, 403–414.
5. A. Tardieu, S. Finet, and F. Bonneté, *Journal of Crystal Growth*, 2001, **232**, 1–9.
6. J. Narayanan and X. Y. Liu, *Biophysical Journal*, 2003, **84**, 523–532.
7. P. M. Tessier, A. M. Lenhoff, and S. I. Sandler, *Biophysical Journal*, 2002, **82**, 1620–1631.
8. F. Bonneté, N. Ferte, J. P. Astier, and S. Veesler, *J. Phys. IV France*, 2004, **118**, 3–13.
9. M. Muschol and F. Rosenberger, *J Chem Phys*, 1997, **107**, 1953.
10. F. Zhang, M. Skoda, R. Jacobs, S. Zorn, R. Martin, C. Martin, G. Clark, S. Weggler, A. Hildebrandt, O. Kohlbacher, and F. Schreiber, *Phys. Rev. Lett.*, 2008, **101**, 148101.
11. M. Malfois, F. Bonneté, L. Belloni, and A. Tardieu, *J Chem Phys*, 1996, **105**, 3290–3300.

12. A. C. Dumetz, A. M. Chockla, E. W. Kaler, and A. M. Lenhoff, *Biophysical Journal*, 2008, **94**, 570–583.

13. F. Zhang, R. Roth, M. Wolf, F. Roosen-Runge, M. W. A. Skoda, R. M. J. Jacobs, M. Stzucki, and F. Schreiber, *Soft Matter*, 2012, **8**, 1313.

14. D. I. Svergun and M. H. J. Koch, *Reports on Progress in Physics*, 2003, **66**, 1735–1782.

15. D. I. Svergun, M. H. J. Koch, P. A. Timmins, and R. P. May, *Small Angle X-Ray and Neutron Scattering from Solutions of Biological Macromolecules*, Oxford University Press, 2013.

16. V. K. Kelkar, J. Narayanan, and C. Manohar, *Langmuir*, 1992, **8**, 2210–2214.

17. M. Niebuhr and M. H. J. Koch, *Biophysical Journal*, 2005, **89**, 1978–1983.

18. N. Javid, K. Vogtt, C. Krywka, M. Tolan, and R. Winter, *Phys. Rev. Lett.*, 2007, **99**, 028101.

19. M. A. Schroer, J. Markgraf, D. C. F. Wieland, C. J. Sahle, J. Möller, M. Paulus, M. Tolan, and R. Winter, *Phys. Rev. Lett.*, 2011, **106**, 178102.

20. J. Möller, M. A. Schroer, M. Erlkamp, S. Grobelny, M. Paulus, S. Tiemeyer, F. J. Wirkert, M. Tolan, and R. Winter, *Biophysical Journal*, 2012, **102**, 2641–2648.

21. A. J. Chinchalikar, V. K. Aswal, J. Kohlbrecher, and A. G. Wagh, *Phys. Rev. E*, 2013, **87**, 062708.

22. B. V. Derjaguin, *Theory of stability of colloids and thin films*, Plenum Publishers, 1989.

23. E. J. W. Verwey and J. T. G. Overbeek, *Theory of the Stability of Lyophobic Colloids*, Courier Dover Publications, 1999.

24. H. Imamura, T. Morita, T. Sumi, Y. Isogai, M. Kato, and K. Nishikawa, *J Synchrotron Radiat*, 2013, **20**, 919–922.

25. T. Fukasawa and T. Sato, *Phys Chem Chem Phys*, 2011, **13**, 3187–3196.

26. D. N. Petsev and P. G. Vekilov, *Phys. Rev. Lett.*, 2000.

27. F. Zhang, M. W. A. Skoda, R. M. J. Jacobs, R. A. Martin, C. M. Martin, and F. Schreiber, *J Phys Chem B*, 2007, **111**, 251–259.

28. M. L. Broide, T. M. Tominc, and M. D. Saxowsky, *Phys. Rev. E*, 1996, **53**, 6325–6335.

29. G. Fritz, *The Journal of Chemical Physics*, 2006, **124**, 214707–214707.

30. J.-P. Hansen and I. R. McDonald, *Theory of simple liquids; 2nd ed*, Academic Press, London, 1990.

31. L. Verlet, *Molecular Physics*, 1980, **41**, 183–190.

32. N. Choudhury and S. K. Ghosh, *J Chem Phys*, 2002, **116**, 8517.

33. D. E. Kuehner, J. Engmann, F. Fergg, M. Wernick, H. W. Blanch, and J. M. Prausnitz, *J Phys Chem B*, 1999, **103**, 1368–1374.

34. A. Stradner, H. Sedgwick, F. Cardinaux, W. C. K. Poon, S. U. Egelhaaf, and P. Schurtenberger, *Nature*, 2004, **432**, 492–495.

35. A. Shukla, E. Mylonas, E. Di Cola, S. Finet, P. Timmins, T. Narayanan, and D. I. Svergun, *Proc. Natl. Acad. Sci. U.S.A.*, 2008, **105**, 5075–5080.

36. T. Sumi, H. Imamura, T. Morita, and K. Nishikawa, *Journal of Molecular Liquids*, 2014.

37. T. Sumi and H. Sekino, *J Chem Phys*, 2007, **126**, 144508.

38. Y. Liu, W.-R. Chen, and S.-H. Chen, *The Journal of Chemical Physics*, 2005, **122**, 44507–44507.

39. F. Cardinaux, A. Stradner, P. Schurtenberger, F. Sciortino, and E. Zaccarelli, *EPL (Europhysics Letters)*, 2007, **77**, 48004.

40. M. Muschol and F. Rosenberger, *J Chem Phys*, 1997, **107**, 1953.

41. G. A. Vliegenthart and H. N. W. Lekkerkerker, *J Chem Phys*, 2000, **112**, 5364.

42. J. Möller, S. Grobelny, J. Schulze, S. Bieder, A. Steffen, M. Erlkamp, M. Paulus, M. Tolan, and R. Winter, *Phys. Rev. Lett.*, 2014, **112**, 028101.

43. F. Zhang, R. Roth, M. Wolf, F. Roosen-Runge, M. W. A. Skoda, R. M. J. Jacobs, M. Stzucki, and F. Schreiber, *Soft Matter*, 2012, **8**, 1313.

44. P. R. T. Wolde, *Science*, 1997, **277**, 1975–1978.

45. S. Brandon, P. Katsonis, and P. Vekilov, *Phys. Rev. E*, 2006, **73**, 061917.

46. F. Zhang, F. Roosen-Runge, A. Sauter, R. Roth, M. W. A. Skoda, R. M. J. Jacobs, M. Sztucki, and F. Schreiber, *Faraday Discuss.*, 2012, **159**, 313.